

## Traffic of single-headed motor proteins KIF1A: Effects of lane changing

Debashish Chowdhury,<sup>1,\*</sup> Ashok Garai,<sup>1,†</sup> and Jian-Sheng Wang<sup>2,‡</sup>

<sup>1</sup>Department of Physics, Indian Institute of Technology, Kanpur 208016, India

<sup>2</sup>Department of Physics, National University of Singapore, Singapore 117542, Singapore

(Received 7 March 2008; revised manuscript received 18 April 2008; published 12 May 2008)

KIF1A kinesins are single-headed motor proteins which move on cylindrical nanotubes called microtubules (MTs). A normal MT consists of 13 protofilaments on which the equispaced motor binding sites form a periodic array. The collective movement of the kinesins on a MT is, therefore, analogous to vehicular traffic on multilane highways where each protofilament is the analog of a single lane. Does lane changing increase or decrease the motor flux per lane? We address this fundamental question here by appropriately extending a recent model [P. Greulich *et al.*, Phys. Rev. E **75**, 041905 (2007)]. By carrying out analytical calculations and computer simulations of this extended model, we predict that the flux per lane can increase or decrease with the increasing rate of lane changing, depending on the concentrations of motors and the rate of hydrolysis of ATP, the “fuel” molecules. Our predictions can be tested, in principle, by carrying out *in vitro* experiments with fluorescently labeled KIF1A molecules.

DOI: [10.1103/PhysRevE.77.050902](https://doi.org/10.1103/PhysRevE.77.050902)

PACS number(s): 87.16.ad, 87.16.Nn

Members of the kinesin superfamily of motor proteins move along microtubules (MTs), which are cylindrical nanotubes [1,2]. A normal MT consists of 13 protofilaments, each of which is formed by the head-to-tail sequential lining up of basic subunits. Each subunit of a protofilament is an 8 nm heterodimer of  $\alpha$ - $\beta$  tubulins and provides a specific binding site for a single head of a kinesin motor. Often many kinesins move simultaneously along a given MT; because of close similarities with vehicular traffic [3], the collective movement of the molecular motors on a MT is sometimes referred to as molecular motor traffic [4–8].

The effects of lane changing on the flow properties of vehicular traffic has been investigated extensively using particle-hopping models [3] which are, essentially, appropriate extensions of the totally asymmetric simple exclusion process (TASEP) [9–11]. Models of multilane TASEP, where the particles can occasionally change lanes, have also been investigated analytically [12,13]. Two-lane generalizations of generic models of cytoskeletal molecular motor traffic have also been reported [14,15].

Recently a quantitative theoretical model has been developed [16,17] (from now onward, we shall refer to it as the NOSC model) for the traffic of KIF1A proteins, which are single-headed kinesins [18–20], by explicitly capturing the essential features of the mechanochemical cycle of each individual KIF1A motor, in addition to their steric interactions. In this Rapid Communication we extend the NOSC model by adding to the master equation all those terms which correspond to lane changing. Solving these equations analytically, we address a fundamental question: Does lane changing increase or decrease flux per lane? We show that the answer to this question depends on the parameter regime of our model. We establish the levels of accuracy of our analytical results by comparing with the corresponding numerical data ob-

tained from computer simulations of the model. We interpret the results physically and suggest experiments for testing our theoretical predictions.

The equispaced binding sites for KIF1A on a given protofilament of the MT are labeled by the integer index  $i$  ( $i=1, \dots, L$ ). We use the integer index  $j$  to label the protofilaments; the position of each binding site is denoted completely by the pair  $(i, j)$ . Because of the tubular geometry of the MT, periodic boundary conditions along the  $j$  direction would be a natural choice. We impose periodic boundary conditions also along the  $i$  direction, as it not only simplifies our analytical calculations but is also adequate to answer the fundamental questions that we address in this Rapid Communication.

In each mechanochemical cycle a KIF1A motor hydrolyzes one molecule of adenosine triphosphate (ATP) which supplies the mechanical energy required for its movement.

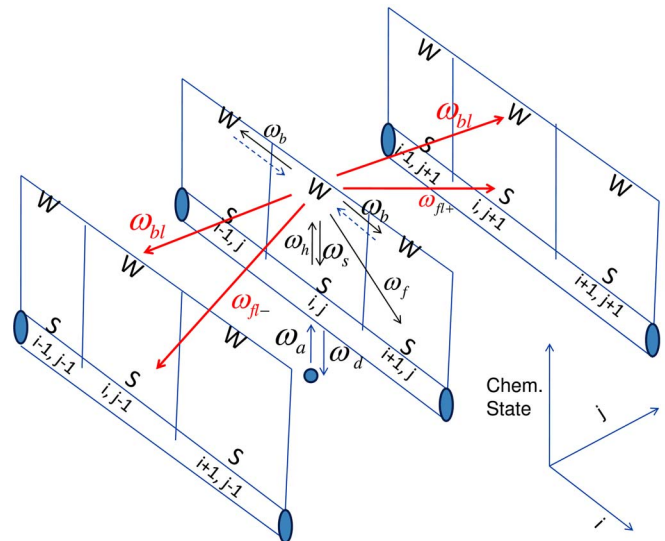


FIG. 1. (Color online) A schematic representation of our model, together with the allowed transitions and the corresponding rate constants.

\*debch@iitk.ac.in

†garai@iitk.ac.in

‡phywjs@nus.edu.sg

The experimental results on KIF1A motors [18–20] indicate that a simplified description of its mechanochemical cycle in terms of a two-state model [16] would be sufficient to understand their traffic on a MT. In the two “chemical” states labeled by the symbols  $S$  and  $W$  the motor is, respectively, strongly and weakly bound to the MT.

In the NOSC model, a KIF1A molecule is allowed to attach to (and detach from) a site with rates  $\omega_a$  (and  $\omega_d$ ). The rate constant  $\omega_b$  corresponds to the unbiased Brownian motion of the motor in the state  $W$ . The rate constant  $\omega_h$  is associated with the process driven by ATP hydrolysis, which causes the transition of the motor from the state  $S$  to the state  $W$ . The rate constants  $\omega_f$  and  $\omega_s$ , together, capture the Brownian ratchet mechanism [21,22] of a KIF1A motor. Moreover, any movement of the motor under these rules is, finally, implemented only if the target site is not already occupied by another motor.

The rules of time evolution in the extended NOSC model proposed here are identical to those in the NOSC model, except for the following additional lane-changing rules (see Fig. 1):

A motor weakly bound (i.e., in state  $W$ ) to the binding site  $i$  on the protofilament  $j$  is allowed to move to the positions  $(i, j+1)$  and  $(i, j-1)$

(i) *without* simultaneous change in its chemical state, both the corresponding rates being  $\omega_b$ ;

(ii) *with* simultaneous transition to the chemical state  $S$ , the corresponding rate constants being  $\omega_{fl+}$  and  $\omega_{fl-}$ , respectively.

Let  $S_i(j, t)$  and  $W_i(j, t)$  denote the probabilities for a motor to be in the “chemical” states  $S$  and  $W$ , respectively, at site  $i$  on the protofilament  $j$ . In the extended NOSC model, under mean-field approximation, the master equations for the probabilities  $S_i(j, t)$  and  $W_i(j, t)$  are given by

$$\begin{aligned} \frac{dS_i(j, t)}{dt} = & \omega_a[1 - S_i(j, t) - W_i(j, t)] - \omega_h S_i(j, t) - \omega_d S_i(j, t) \\ & + \omega_s W_i(j, t) + \omega_f W_{i-1}(j, t)[1 - S_i(j, t) - W_i(j, t)] \\ & + \omega_{fl+}[W_i(j-1, t)][1 - S_i(j, t) - W_i(j, t)] \\ & + \omega_{fl-}[W_i(j+1, t)][1 - S_i(j, t) - W_i(j, t)], \end{aligned} \quad (1)$$

$$\begin{aligned} \frac{dW_i(j, t)}{dt} = & \omega_h S_i(j, t) - \omega_s W_i(j, t) - \omega_f W_i(j, t)[1 - S_{i+1}(j, t) - W_{i+1}(j, t)] \\ & - \omega_b W_i(j, t)[2 - S_{i+1}(j, t) - W_{i+1}(j, t) - S_{i-1}(j, t) - W_{i-1}(j, t)] + \omega_b[W_{i-1}(j, t) + W_{i+1}(j, t)][1 - S_i(j, t) - W_i(j, t)] \\ & + \omega_{fl+}[W_i(j-1, t) + W_i(j+1, t)][1 - S_i(j, t) - W_i(j, t)] - \omega_{fl-} W_i(j, t)[2 - S_i(j+1, t) - W_i(j+1, t) - S_i(j-1, t) - W_i(j-1, t)] \\ & - \omega_{fl+} W_i(j, t)[1 - S_i(j+1, t) - W_i(j+1, t)] - \omega_{fl-} W_i(j, t)[1 - S_i(j-1, t) - W_i(j-1, t)]. \end{aligned} \quad (2)$$

In the steady state under *periodic* boundary conditions,  $\tilde{S} = S_i(j, t)$  and  $\tilde{W} = W_i(j, t)$ , independent of  $t$  and irrespective of  $i$  and  $j$ ; from Eqs. (1) and (2), we get

$$\tilde{S} = \frac{-\tilde{\Omega}_h - \tilde{\Omega}_s - (\tilde{\Omega}_s - 1)K + \sqrt{\tilde{D}}}{2K(1+K)} \quad (3)$$

$$\tilde{W} = \frac{\tilde{\Omega}_h + \tilde{\Omega}_s + (\tilde{\Omega}_s + 1)K - \sqrt{\tilde{D}}}{2K}, \quad (4)$$

where  $K = \omega_d / \omega_a$ ,  $\tilde{\Omega}_h = \omega_h / \tilde{\omega}_f$ ,  $\tilde{\Omega}_s = \omega_s / \tilde{\omega}_f$ , with  $\tilde{\omega}_f = \omega_f + \omega_{fl+} + \omega_{fl-}$ , and

$$\tilde{D} = 4\tilde{\Omega}_s K(1+K) + (\tilde{\Omega}_h + \tilde{\Omega}_s + (\tilde{\Omega}_s - 1)K)^2. \quad (5)$$

The average total density of the motors attached to each filament of the MT in the steady state is given by

$$\rho = \tilde{S} + \tilde{W} = \frac{\tilde{\Omega}_h + \tilde{\Omega}_s + (\tilde{\Omega}_s + 1)K - \sqrt{\tilde{D}} + 2}{2(1+K)}. \quad (6)$$

Using the expressions (3) and (4) for  $\tilde{S}$  and  $\tilde{W}$ , respectively, in the expression

$$J = \omega_f \tilde{W}(1 - \tilde{S} - \tilde{W}) \quad (7)$$

for the flux of KIF1A motors per lane of the MT highway, we get

$$J = \frac{\omega_f [K^2 - (\tilde{\Omega}_h + (1+K)\tilde{\Omega}_s - \sqrt{\tilde{D}})^2]}{4K(1+K)}. \quad (8)$$

For graphical presentation of our main results, we use the estimates of the rate constants, listed in Table I, which were extracted earlier [17] from empirical data on single KIF1A (we use  $\omega_h = 125 \text{ s}^{-1}$ ). Since no estimate of  $\omega_{fl+}$  and  $\omega_{fl-}$  are

TABLE I. Rate constants of the NOSC model which have been extracted from empirical data on single KIF1A experiments [17].

Rate constant	Numerical value/range ( $\text{s}^{-1}$ )
$\omega_a$	0.1–10.0
$\omega_d$	0.1
$\omega_h$	0–250
$\omega_s$	145
$\omega_f$	55

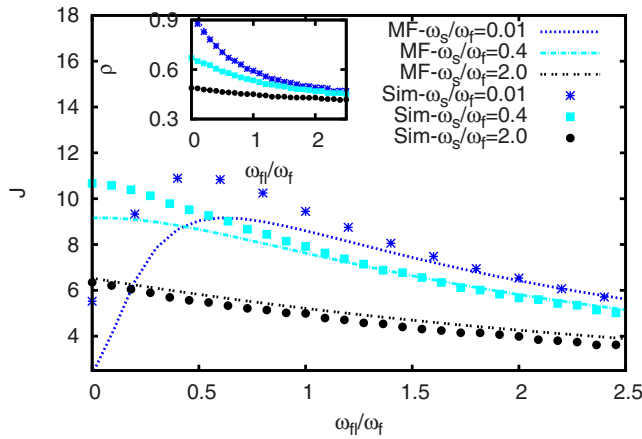


FIG. 2. (Color online) Flux per lane (and, in the inset, average density of the motors on each lane) are plotted against  $\omega_{fl}/\omega_f$  for a few values of  $\omega_s/\omega_f$ . Our mean-field predictions (labeled MF) are plotted by lines while the discrete data points (labeled Sim) have been obtained from our computer simulations of the model.

available, we use  $\omega_{fl+} = \omega_{fl-} = \omega_{fl}$  and vary the single parameter  $\omega_{fl}/\omega_f$  over a wide range to explore the consequences of different rates of lane changing. The flux per lane [obtained from (8)] and the average density  $\rho$  [given by (6)] are plotted against  $\omega_{fl}/\omega_f$  in Fig. 2 for several different values of  $\omega_s/\omega_f$  and compared with the corresponding simulation data.

Recall that flux is essentially an average of the product of the density and speed of the motors. For sufficiently high  $\omega_s/\omega_f$ , the density  $\rho$  is small even in the absence of lane changing ( $\omega_{fl}=0$ ) and, consequently, the motors feel hardly any steric hindrance; increasing  $\omega_{fl}/\omega_f$  in this regime of  $\omega_s/\omega_f$  has very little effect on the average speed of the motors and it is the decreasing density that is responsible for the *monotonic* decrease of  $J$  with  $\omega_{fl}$ .

In sharp contrast, at sufficiently low values of  $\omega_s/\omega_f$ ,  $J$  varies *nonmonotonically* with  $\omega_{fl}/\omega_f$ . In this regime of  $\omega_s/\omega_f$ , at  $\omega_{fl}=0$ , the high density of  $\rho$  causes steric hindrances which, in turn, lead to small  $J$ . When  $\omega_{fl}$  is “switched on,”  $\rho$  decreases with increasing  $\omega_{fl}$  and  $J$  increases up to a maximum because of the weakening of the hindrance effects. But, beyond a certain range of  $\omega_{fl}/\omega_f$ , the density of motors becomes so low that the movement of the motors is practically free of mutual hindrance; the decrease of  $J$  beyond its maximum is caused by the further reduction of density. The larger difference between the predictions of our approximate analytical calculations and computer simulation data at lower values of  $\omega_s/\omega_f$  arises from the fact that the mean-field approximation neglects correlations that increase with increasing density of the motors.

The above interpretation of trends of variations of  $J$  in Fig. 2 in terms of the corresponding variation of  $\rho$  is consistent with the results shown in Figs. 3 and 4. But, why does  $\rho$  decrease monotonically with increasing  $\omega_{fl}/\omega_f$ ? Increasing  $\omega_{fl}$ , keeping all the other rate constants unaltered, leads to a higher overall rate of transitions into strongly bound states. Since detachments of the motors from the microtubule track take place from the strongly bound state (see Ref. [23]), the steady-state density is lower for higher values of  $\omega_{fl}/\omega_f$ .

An approximate expression for  $J$ , which is obtained by

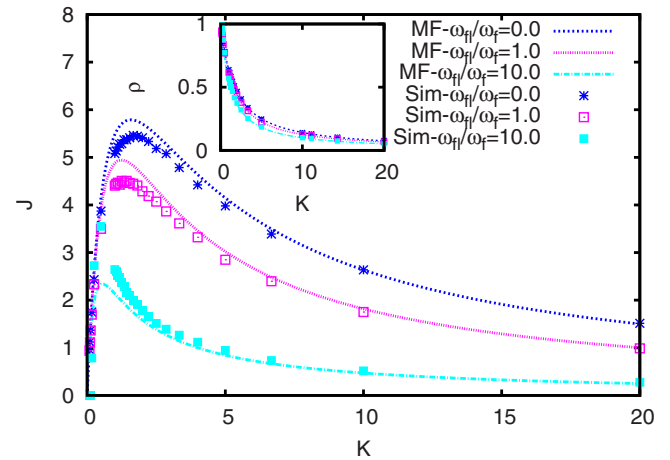


FIG. 3. (Color online) Same as in Fig. 2, except that the data are plotted against  $K$  for a few values of  $\omega_{fl}/\omega_f$ .

retaining only the terms up to the first order in  $\omega_{fl}$  in a Taylor expansion of the right hand side of (8), is given by

$$J = J_0 - 4 \left( \frac{\omega_{fl}}{\omega_f} \right) J_0 + \left( \frac{\omega_{fl}}{2\sqrt{D}(1+K)} \right) \times \left( [(1+K)\Omega_s + K]^2 + [(1+K)\Omega_s - \sqrt{D}]^2 - [\Omega_h - \sqrt{D}]^2 - [\Omega_h - K]^2 \right) + O(\omega_{fl}^2), \quad (9)$$

where  $J_0$  is the flux corresponding to  $\omega_{fl}=0$  (i.e., in the absence of lane changing). The approximate formula (9) still provides a reasonably good estimate of the flux even when  $\omega_{fl}$  is as large as  $\omega_f$ .

In this Rapid Communication we have extended the NOSC model for KIF1A traffic on MTs [16,17] by incorporating processes which correspond to shifting of the motors from one protofilament to another. These processes are analogous to lane changing of vehicles on multilane highways. On the basis of analytical treatment and computer simulations of the extended NOSC model, we have predicted the effects of such lane changing on  $J$ , the steady-state flux

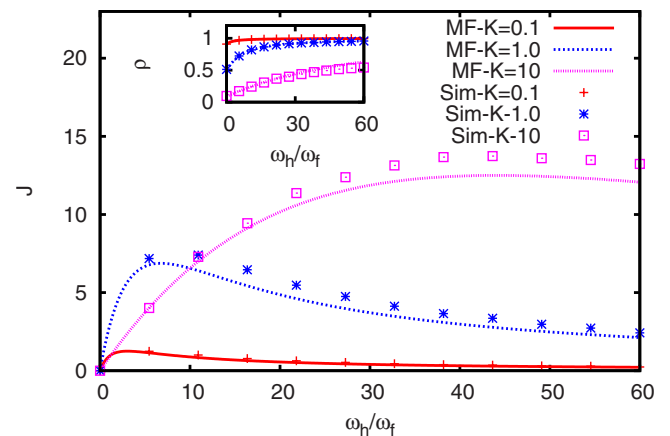


FIG. 4. (Color online) Same as in Fig. 2, except that the data are plotted against  $\omega_h/\omega_f$  for a few values of  $K$ .

of the KIF1A motors per lane. Over a wide region of parameter space,  $J$  decreases monotonically with an increasing value of  $\omega_{fl}$ , a rate constant for lane changing. However, in some regions of parameter space,  $J$  varies *nonmonotonically* with increasing  $\omega_{fl}$ . We have interpreted the results by correlating the observed trends of variation of  $J$  with the corresponding variation of  $\rho$ , the average density of motors on a lane, and establishing the dependence of  $\rho$  on  $\omega_{fl}$ .

Double-headed conventional kinesin rarely changes lanes [24]. Double-headed dyneins may change lanes *in vitro* [25,26] but, perhaps, not *in vivo* [27]. The bound head of a double-headed motor imposes constraints on the stepping of the unbound head. Since such constraints do not exist for

single-headed kinesins, KIF1A may find it easier to change lanes. However, KIF1A may dimerize *in vivo* [28]. Therefore, *in vitro* experiments with fluorescently labeled KIF1A would be able to test our theoretical predictions. In particular, variations of  $J$  with  $K$  and  $\omega_h$  (see Figs. 3 and 4) can be probed by varying the concentration of KIF1A and ATP molecules, respectively, in the solution.

We thank J. Howard, R. Mallik, A. Schadschneider, and G. Schütz for useful suggestions. This work was supported by the NUS-India Research Initiatives, a Faculty Research Grant (NUS), a CSIR Research Grant (India), and the Physics Department of NUS and NUS-IITK MoU.

- 
- [1] *Molecular Motors*, edited by M. Schliwa (Wiley-VCH, 2003).
- [2] J. Howard, *Mechanics of Motor Proteins and the Cytoskeleton* (Sinauer Associates, Sunderland, 2001).
- [3] D. Chowdhury, L. Santen, and A. Schadschneider, Phys. Rep. **329**, 199 (2000).
- [4] D. Chowdhury, A. Schadschneider, and K. Nishinari, Phys. Life. Rev. **2**, 318 (2005).
- [5] R. Lipowsky, S. Klumpp, and T. M. Nieuwenhuizen, Phys. Rev. Lett. **87**, 108101 (2001); R. Lipowsky *et al.*, Physica A **372**, 34 (2006), and references therein.
- [6] A. Parmeggiani, T. Franosch, and E. Frey, Phys. Rev. Lett. **90**, 086601 (2003); Phys. Rev. E **70**, 046101 (2004).
- [7] M. R. Evans, R. Juhasz, and L. Santen, Phys. Rev. E **68**, 026117 (2003).
- [8] V. Popkov, A. Rákos, R. D. Willmann, A. B. Kolomeisky, and G. M. Schütz, Phys. Rev. E **67**, 066117 (2003).
- [9] B. Schmittmann and R. K. P. Zia, in *Phase Transition and Critical Phenomena*, edited by C. Domb and J. L. Lebowitz (Academic, New York, 1995), Vol. 17.
- [10] B. Derrida, Phys. Rep. **301**, 65 (1998).
- [11] G. M. Schütz, *Phase Transitions and Critical Phenomena* (Academic, New York, 2001), Vol. 19.
- [12] E. Pronina and A. B. Kolomeisky, J. Phys. A **37**, 9907 (2004); Physica A **372**, 12 (2006).
- [13] T. Mitsudo and H. Hayakawa, J. Phys. A **38**, 3087 (2005).
- [14] R. Wang *et al.*, e-print arXiv:q-bio/0703043v1.
- [15] T. Reichenbach, T. Franosch, and E. Frey, Phys. Rev. Lett. **97**, 050603 (2006); T. Reichenbach, E. Frey, and T. Franosch, New J. Phys. **9**, 159 (2007).
- [16] K. Nishinari, Y. Okada, A. Schadschneider, and D. Chowdhury, Phys. Rev. Lett. **95**, 118101 (2005).
- [17] P. Greulich, A. Garai, K. Nishinari, A. Schadschneider, and D. Chowdhury, Phys. Rev. E **75**, 041905 (2007).
- [18] Y. Okada and N. Hirokawa, Science **283**, 1152 (1999); Proc. Natl. Acad. Sci. U.S.A. **97**, 640 (2000).
- [19] Y. Okada, H. Higuchi, and N. Hirokawa, Nature (London), **424**, 574 (2003).
- [20] R. Nitta *et al.*, Science **305**, 678 (2004).
- [21] F. Jülicher, A. Ajdari, and J. Prost, Rev. Mod. Phys. **69**, 1269 (1997).
- [22] P. Reimann, Phys. Rep. **361**, 57 (2002).
- [23] The terminology “strongly bound” and “weakly bound” states, still used for historical reasons, is misleading; actually, the active detachment of KIF1A from the MT track takes place while in a transient intermediate state during the transition from the “strongly bound” state to the “weakly bound” state [20].
- [24] S. Ray *et al.*, J. Cell Biol. **121**, 1083 (1993).
- [25] Z. Wang, S. Khan, and M. P. Sheetz, Biophys. J. **69**, 2011 (1995).
- [26] S. L. Reck-Peterson *et al.*, Cell **126**, 335 (2006).
- [27] T. Watanabe *et al.*, Biochem. Biophys. Res. Commun. **359**, 1 (2007).
- [28] M. Tomishige, D. R. Klopfenstein, and R. D. Vale, Science **297**, 2263 (2002).